^{55}Mn NMR and magnetization studies of $La_{0.67}Sr_{0.33}MnO_3$ thin films

A. A. Sidorenko,* G. Allodi, and R. De Renzi
Dipartimento di Fisica e Unità CNISM di Parma, Università degli Studi di Parma, Viale delle Scienze, 7A, 43100 Parma, Italy

G. Balestrino and M. Angeloni
INFM-COHERENTIA, Dipartimento di Ingegneria Meccanica, Università di Roma Tor Vergata, Via del Politecnico, 1, 00133 Roma, Italy

(Received 26 July 2005; revised manuscript received 19 October 2005; published 3 February 2006)

^{55}Mn nuclear magnetic resonance and magnetization studies of the series of $La_{0.67}Sr_{0.33}MnO_3$ thin films have been performed at low temperature. Two distinct lines were observed, at 322 MHz and 380 MHz, corresponding to two different phases, the former located at the interface, with localized charges, and the latter corresponding to the film bulk, with itinerant carriers (as it was also found in Ca manganite films). The spin-echo amplitude was measured as a function of a dc magnetic field applied either in the film plane or perpendicular to it. The field dependence of the NMR signal intensity above the effective anisotropy field agrees well with a model of magnetically homogeneous sample. The enhanced magnetic anisotropy estimated for the NMR signal from the interface is consistent with its very small thickness, indicating similar magnetic properties in charge localized and itinerant regions.

DOI: 10.1103/PhysRevB.73.054406 PACS number(s): 76.60.−k, 75.70.−i, 75.30.Gw

I. INTRODUCTION

Recently, numerous experiments have revealed a profound effect of substrate on both transport and magnetic properties of epitaxial thin films $La_{0.67}M_{0.33}MnO_3$ (M=Sr, Ca, or Ba) which are ferromagnetic metals at low temperatures and paramagnetic insulators at high temperatures. In the manganite films, the substrate-induced strain affects magnetoresistivity,[1–3] Curie temperature,[4] and magnetic microstructure.[5,6]In particular, the magnetic anisotropy energy in the thin manganite films strongly depends on strain and, therefore, on the substrate material, film thickness, and deposition parameters.[7–9] For instance, whereas the $La_{0.67}Ca_{0.33}MnO_3$ films grown on $SrTiO_3$ substrate were found to have uniaxial magnetic anisotropy (hard axis/easy plane) with easy plane being the film plane, the possibility of producing strained manganite films deposited on $LaAlO_3$ substrate with the easy magnetization axis along film normal has been proposed.[10] In addition, nuclear magnetic resonance (NMR) studies on a series of the epitaxial thin films discovered the existence of a complex phase separation phenomenon,[11] correlated to the insulating nature of the thinner films,[12,13] that may reflect an intrinsic property of film-substrate interface. The material engineering potentials of this phenomenon, which might appear at first sight a drawback for oxide materials, were recently demonstrated by an example of successful tailoring of this interface property.[14]

It is therefore of crucial importance for future applications in tunneling magnetoresistive devices to characterize the origin of the strong film-substrate interactions. In this paper ^{55}Mn NMR and magnetization data are used in order to correlate the microscopic and macroscopic properties of the manganite $La_{0.67}Sr_{0.33}MnO_3/SrTiO_3$ interfaces. The rest of the paper is divided into Sec. II on material preparation and experimental techniques; Sec. III on NMR and magnetization results, including discussion of a simple model; and Sec. IV with our conclusions.

II. MATERIALS AND EXPERIMENTS

Epitaxial $La_{0.67}Sr_{0.33}MnO_3$ (LSMO) films with thickness varying from 8 to 500 nm were grown on (100) $SrTiO_3$ (STO) substrates using the pulsed laser deposition technique. X-ray diffraction experiments show that the LSMO thin films exhibit a cube-on-cube type of epitaxial arrangement on the substrates. Deposition conditions, structural characterization, and transport properties have been described elsewhere.[4] It should be mentioned here that the annealing duration for optimal oxygen content was found to vary with film thickness: two hours for thicker films and half an hour and less for thinner films.

For NMR experiments the home-built broadband fast-averaging spectrometer HyReSpect[15] was used. Two types of NMR experiments are presented in this paper, both performed at T=1.6 K. The zero-field spectra were obtained in the frequency range 300–450 MHz by means of a standard optimized Θ-τ-Θ spin-echo pulse sequence, plotting point by point the amplitude at zero frequency shift of the fast Fourier transform of each echo as a function of transmission frequency. The plotted data are always corrected for the NMR sensitivity, dividing amplitudes by ω^2 and by the evaluated enhancement factor η.

The field-swept NMR measurements were taken at fixed frequency with the same sequence in a static magnetic field **H** ranging from zero to 20 kOe, applied either parallel or perpendicular to the film surface. The radio frequency field **h** was parallel to the film plane, and always orthogonal to **H**. In order to ensure that the sample was initially in a single domain state, we started from saturation and measured the NMR signal varying the magnetic field intensity H along a full hysteresis loop.

In ferromagnetic materials, the response of the nuclei to an applied resonance radio-frequency field **h** is amplified by the electronic enhancement factor η. Two mechanisms of

enhancement may typically be distinguished in homogeneous ferromagnets. One is due to the rf-induced motion of the domain walls;[16,17] it is generally dominant in zero field and obviously removed by the application of a static field approaching the saturation value. The other mechanism, which is usually less effective by one to two orders of magnitude, arises from the rotation of the magnetization in the bulk of domains, and it comes into play both in zero and in an applied field. The corresponding domain enhancement factor can be related to the local field at the nucleus $\mathbf{H_n}$ and the effective magnetic anisotropy by a simple theoretical model.[16] Therefore, the magnetic anisotropy of films can be studied by measuring both the NMR intensity and the shift of the resonance frequency as a function of the field, once sufficiently large field has been applied to ensure that all the domain walls have been swept out.

Axial magnetization was measured by using a commercial superconducting quantum interference device (SQUID), 5 T quantum MPMS, at $T=2$ K and in the 0–30 kOe field range, both with the field parallel and perpendicular to the film surface. We avoided spurious contributions to the measured signal, other than from the film and the substrate, by using diamagnetic sample holders with uniform mass and magnetic moment distribution along the whole SQUID scanning length. The magnetization data of the manganite films were corrected for the observed diamagnetic contribution of the substrate. The maximum fields misalignment in both NMR and SQUID measurements was estimated to be of the order of 5°.

III. RESULTS AND DISCUSSION

A. Zero-field ^{55}Mn NMR

In the mixed valence manganites, different manganese states yield distinct contributions to the NMR spectra. The localized Mn^{4+} state gives rise to a peak between 310 and 330 MHz.[18–21] The localized Mn^{3+} resonance strongly depends on the local spin and orbital directions. Its spectral position was shown to vary between 250 MHz and 450 MHz in a Mn ferrimagnetic spinel, in which the spin orientation could be controlled experimentally.[22] The peculiar orbital and spin structure of pseudocubic manganites confines the Mn^{3+} in the range 350–430 MHz, easily distinguished from the Mn^{4+} contribution.[18–21] Finally, the signal corresponding to the Mn^{DE} (double exchange) state from the mixed valence metallic region is associated with a fast hopping of electrons among Mn sites and it shows up as a relatively narrow peak at an intermediate frequency in the 370–400 MHz range.

Zero-field ^{55}Mn NMR spectra obtained at 1.6 K in LSMO/STO films with various thickness are shown in Fig. 1. Two distinct lines at $f^{4+}\approx 322$ MHz and $f^{DE}\approx 380$ MHz, corresponding to two different phases with the localized charges (Mn^{4+} state) and with itinerant carriers (Mn^{DE} state), respectively, are observed. Their origin was already assigned by previous NMR work[11] on $La_{0.67}Ca_{0.33}MnO_3$ to the inhomogeneous separation of a so-called *dead layer*, roughly coinciding with the critical thickness below which the same films appear to be insulating by transport measurements. The dead layer is presumably located at the interface between the substrate and the manganite film. The absence of a corresponding localized Mn^{3+} signal may be attributed to its much faster relaxation rate and possibly to its wider spectral breadth. It should be noted that detailed studies of ultrafine LSMO particles have also revealed the existence of a small contribution from Mn^{4+} state, attributed to the surface of the nanoparticles.[23] Also in that case the corresponding Mn^{3+} signal was missing.

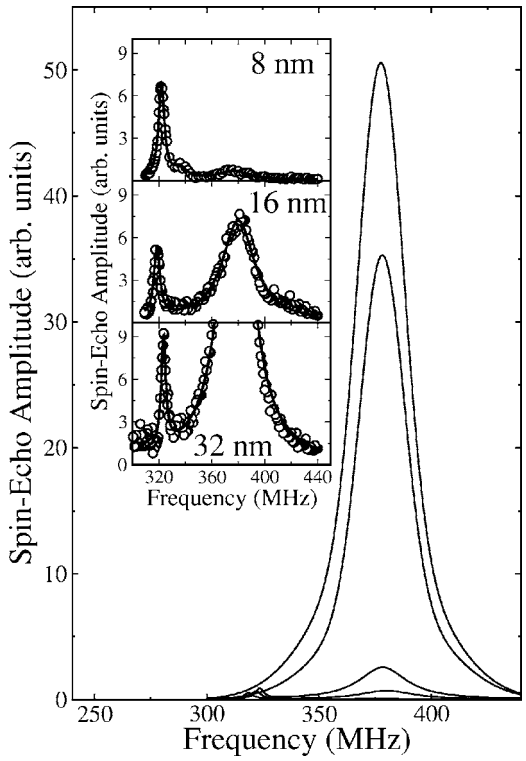

FIG. 1. Zero-field ^{55}Mn spin-echo amplitude measured at 1.6 K in LSMO/STO films with different thicknesses.

As can be seen, the peak intensity at f^{DE} dramatically depends on the film thickness t, whereas the intensity of the peak at f^{4+} is practically unvaried, and, in films with thickness $t\gtrsim 180$ nm, a separate line at f^{4+} is difficult to identify due to overlapping with the strong signal from Mn^{DE}. The values of the integrated spectrum intensity obtained for the $8\leqslant t\leqslant 480$-nm films are plotted as a function of t in Fig. 2(a); within the experimental errors the integrated intensity follows a linear dependence on t, intersecting the horizontal axis at $t_d\approx 4.6\pm 0.5$ nm, as can be seen in the inset. The obtained t_d value is therefore interpreted as the dead-layer thickness and it is comparable with the value 5.3 nm determined on $La_{0.67}Ca_{0.33}MnO_3$.[11] Values of the critical thickness were measured by resistivity in LSMO films on different substrates, yielding comparable results: ~3 nm on (001) $LaAlO_3$ and ~5 nm on (110) $NdGaO_3$.[12] Similar measurements were performed on our films; they confirm the presence of a critical thickness of this order of magnitude.[4]

Figure 2(b) shows the thickness dependence of the applied rf field h required to optimally excite the f^{DE} NMR resonance. The reduction of h with increasing film thickness indicates an increase of the enhancement factor.

In contrast to the NMR study on $La_{0.67}Ca_{0.33}MnO_3$ thin films,[11] a monotonic shift of the f^{DE} peak towards lower

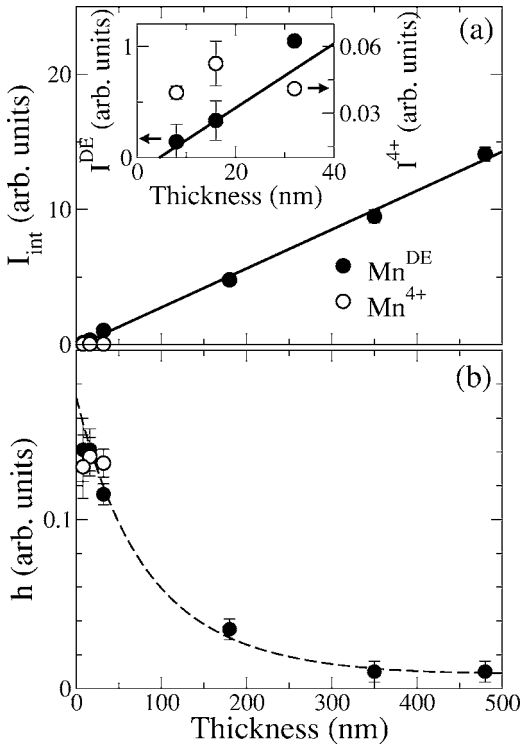

FIG. 2. Thickness dependence at $H=0$ of: (a) the integrated intensity I_{int} of the f^{DE} and of the f^{4+} lines (corrected for thickness dependent enhancement); (b) the applied rf field h, proportional to $1/\eta$ (see text). Inset: Zoom on thiner films.

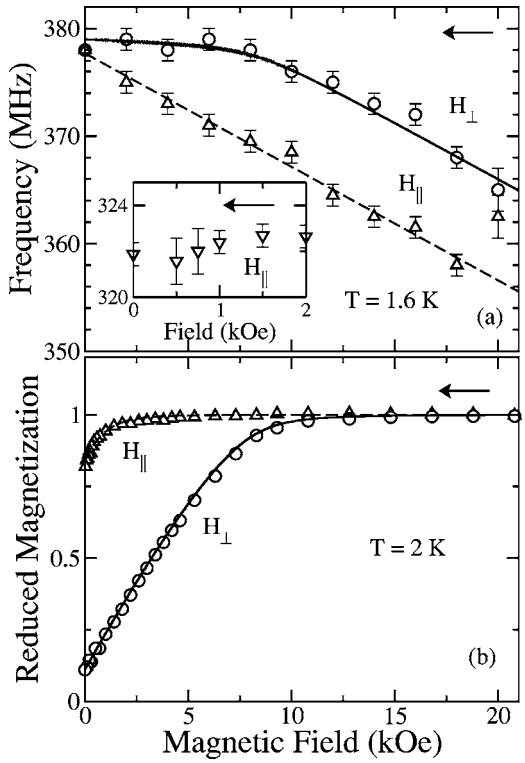

FIG. 3. ^{55}Mn nuclear resonance frequency f^{DE} (a) and the reduced magnetization (b) in the 180-nm thick film as functions of the dc field in the film plane (△) and perpendicular to the film plane (○). The so lid and dashed lines are calculated curves (see text). The inset shows the shift of the f^{4+} resonance line in the 8-nm thick film measured with the field applied in the film plane.

frequency with reduction of the film thickness was not observed for LSMO.

B. Measurements in an applied external field

We shall start by considering the field dependence of the f^{DE} line of the 180-nm thick LSMO/STO film, arising from the metallic region. The experiments were run in two distinct geometries, with the external dc field either in the film plane ($H_\parallel$) or perpendicular to it ($H_\perp$), and with the rf field **h** always in the film plane, at right angles with the dc field.

The field dependent resonance frequency is defined as that corresponding to the maximum amplitude, as determined from the best fit of the Mn^{DE} spectrum to a Lorentzian line shape.

Figure 3(a) shows the shift of the f^{DE} line measured at various dc field up to 20 kOe in both geometries, at $T \approx 1.6$ K. In the $H_\parallel$ geometry (triangles) the resonance spectrum shifts to lower frequencies at a rate close to the Mn magnetogyric ratio $\gamma=1.055$ MHz/kOe. The negative slope indicates that the hyperfine field is negative,[24] that is, it lies antiparallel to the electronic magnetization. When the field is applied perpendicular to the film plane, the demagnetizing field also contributes to the shift in the resonance frequency and in the NMR intensity. As the magnetic field is increased, the demagnetizing field increases up to $4\pi M_s$, and the resonance frequency remains almost independent on the field up to ~8 kOe [Fig. 3(a), circles].

Let us now turn to the f^{DE} echo intensities versus field at fixed frequency. We recall that in homogeneous ferromagnets domain bulk and domain walls give rise to NMR signals distinguished by very different enhancement factors. In low fields the main contribution to the spin-echo intensity is given by the nuclei within the domain walls and its amplitude is expected to decrease with increasing external magnetic field. In intrinsically inhomogeneous materials like the manganites it is not possible to experimentally separate domain-bulk and domain- wall signals by distinguishing their enhancement factors. However, in order to observe a dominant domain-wall contribution the duration and the power of the rf pulses may be fixed at values optimized in zero dc field (ZFO), whereas if both the duration and the power of the rf pulses are adjusted for maximum response at each field (FO, field optimized), a signal is observed also above the effective anisotropy field, where the sample is saturated and the NMR must originate from the bulk of the single domain.

Figure 4(a) displays the field dependences of the spin-echo intensity measured at 1.6 K, $f=380$ MHz, according to the two above-mentioned protocols, for the dc magnetic field applied in the film plane along the hard axis [001]. Both variations of the experiment produce a dramatic reduction of amplitude with field. Since the linewidth (Fig. 1) is quite larger than the shifts [Fig. 3(a)] this amplitude drop is not due to a shift of spectral weight outside the experimental passband. The open squares refer to the ZFO protocol and the signal thus obtained disappears with the application of

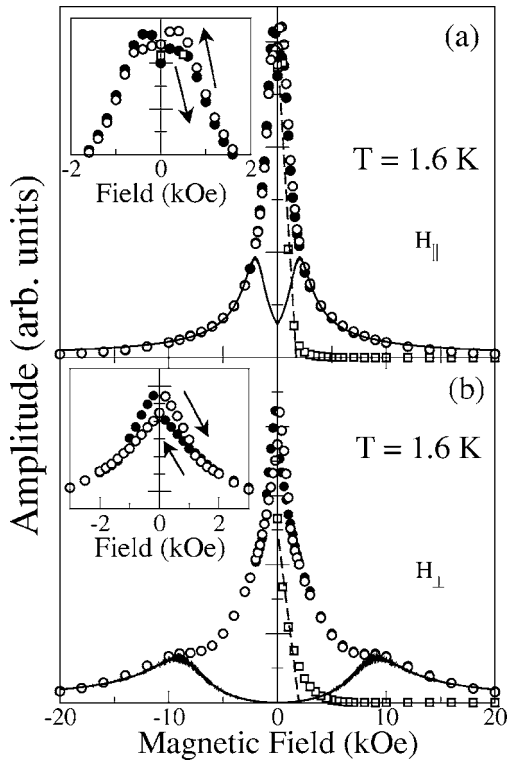

FIG. 4. The spin-echo amplitude at 1.6 K, $f=380$ MHz, for the 180-nm thick film as functions of the dc field in the film plane (a) and perpendicular to the film plane (b), both with the FO (○ decreasing fields, ● increasing fields) and the ZFO (□) protocol. The solid lines represent the calculated curves (see text). The dashed lines are the linear fit. Insets: hysteresis of the NMR amplitude in the vicinity of the zero field.

modest magnetic fields, as domain walls are removed. Assuming that the domain-wall enhancement does not vary dramatically with field, the field dependence of the ZFO signal amplitude reflects approximately the reduction of the domain wall volume.

The FO signal amplitudes were recorded starting from $H_{max}=25$ kOe, in order to ensure a saturated sample, sweeping down the field (open circles) through zero to $-H_{max}$, and then reversing the field sweep direction (closed circles). Notice that in the vicinity of zero field a hysteretic behavior of the amplitude is observed [see the inset of Fig. 4(a)]. The measured spin-echo amplitude peaks at ±200(50) Oe, a value which corresponds to the coercive filed H_c, in agreement with our magnetization data (not shown) and with the literature.[25]

NMR f^{DE} amplitudes were recorded according to both ZFO and FO protocols also for the $H_\perp$ geometry at $f=380$ MHz [Fig. 4(b)]. A behavior similar to that of Fig. 4(a) is obtained for the ZFO curves, whereas the FO signal displays a marked feature around $H\approx 10$ kOe, which roughly corresponds to the demagnetizing field.

The domain-wall nucleation field may be extracted from the ZFO measurements in the assumption that the ZFO signal amplitude is proportional to the total domain wall volume. The *low field* amplitude depends linearly on field (dashed lines in Fig. 4), and the extrapolated values for the

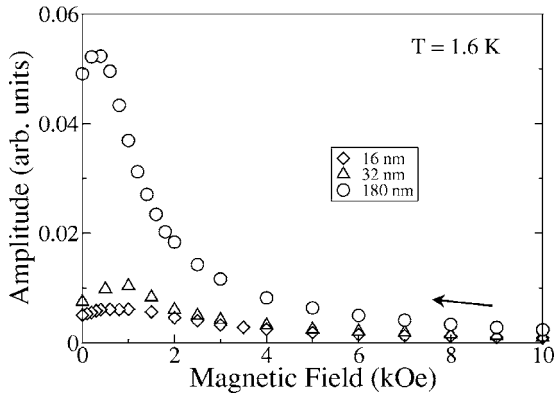

FIG. 5. Field dependence of the spin-echo amplitude at 1.6 K of the manganite films with different thicknesses.

appearance of the domain walls (the intercept at zero amplitude) are 1.73±0.09 kOe and 1.98±0.21 kOe for H applied parallel and perpendicular to the film plane, respectively. However, the actual (internal) nucleation field for the out-of-plane orientation after subtraction of demagnetization is −0.97±0.21 kOe. This negative value, expected in the cubic films[26,27] with magnetic easy axis perpendicular to the film plane, indicates that our 180-nm thick film is fully relaxed and there is no strain induced anisotropy. This also suggests that domain-wall pinning centers are not influential, which is characteristic of a magnetically homogeneous films.[28,29]

It should be noted that the all our films revealed very similar behavior of the spin-echo amplitude versus external magnetic field: Figure 5 shows the FO intensities for two thinner films (32 and 16 nm) together with the 180 nm results of Fig. 4(a).

We turn now to the field dependence of the f^{4+} line, corresponding to the insulating region of the film. Figure 6 represents an evolution of the spin-echo spectra, measured at 1.6 K on the LSMO/STO film with thickness of 8 nm. The three spectra refer to different values of the dc field applied in the film plane. The FO and ZFO protocols coincide for this signal, i.e., the optimal irradiation conditions do not depend on the applied dc field. Furthermore, the enhancement factor is comparable with that of the thinner film f^{DE} line [see Fig. 2(b)].

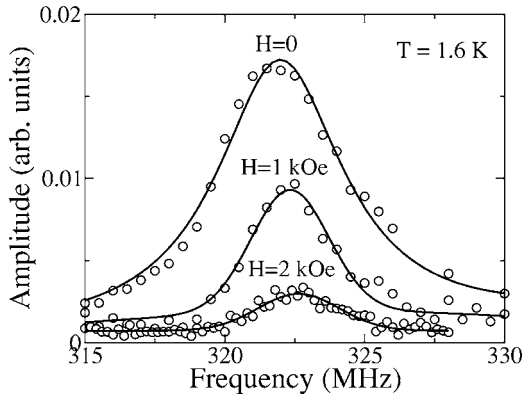

FIG. 6. ^{55}Mn spin-echo spectra at 1.6 K, corresponding to the insulating region of the LSMO/STO film with thickness of 8 nm, for different values of the dc field applied in the film plane.

The NMR signal at $f^{4+} \approx 322$ MHz disappears already in quite weak fields ~ 3 kOe. Since $\eta(H)$ for a single domain drops hyperbolically with field [see Eq. (2) below], the lack of a FO signal at high magnetic fields could just be due to insufficient NMR sensitivity for the very small volume of the dead layer. Vice versa, the Mn^{4+} signal is observed in zero dc field thanks to a large value of $\eta(H=0)$, indicative of the ferromagnetic nature of the insulating region. Notice that the spectra of Fig. 6 do not shift appreciably with the applied field, as it is further confirmed by the inset of Fig. 3(a).

C. Single anisotropy model

For large enough applied fields we can describe our films in a simple single anisotropy model. This is indicated by the shape of the magnetization curve, $M(H)$, measured by SQUID [Fig. 3(b)]. However, FM manganites present intrinsic inhomogeneities even very close to the optimum composition and it is not obvious that such inhomogeneities can be identified from a macroscopic measurement. Therefore, it is interesting to check whether the local microscopic Mn DE probe, which is selective on the electronic configuration of Mn, agrees with the homogeneous picture given by the average magnetic measurement.

We assume a biaxial magnetic anisotropy in the (100) film plane,[5,8] with easy axis along [110], as it was directly checked by SQUID on our film. Hence the total energy for an ideal cubic crystal is given by

$$E = K_1 \sin^2\theta \cos^2\theta - HM_s \cos(\alpha - \theta) - hM_s \cos(\phi + \theta), \tag{1}$$

where θ, ϕ, and α are angles between the easy magnetization axis and the vectors $\mathbf{M}_s$, $\mathbf{h}$, and $\mathbf{H}$, respectively. Then for a resonant excitation of the nuclei in the domain bulk, the theoretical model predicts the following field dependence for the echo amplitude:[16]

$$A(H) = \text{const}\ \frac{\sin^2(\phi + \theta_0)}{(2K_1/M_s)\cos(4\theta_0) + H\cos(-\theta_0)}, \tag{2}$$

where we recall that θ_0 is the angular coordinate of the equilibrium magnetization (an equivalent approach using the perpendicular AC susceptibility is reported in Ref. 30). In order to compare this expression with the experimental data of Fig. 4(a) we need to determine the value of the effective anisotropy field $H_K = 2K_1/M_s$. To this end we employed SQUID on the same film and measured the reduced magnetization M/M_s shown in Fig. 3(b), where the saturation magnetization value $M_s = 620$ emu/cm^3 was determined at 2 K. The reduced magnetization may be fitted to the expression $M/M_s = \cos(\theta_0 - \alpha)$, where the equilibrium angle θ_0 is found by minimizing the energy of Eq. (1) with $h=0$. The dashed line in Fig. 3(b) represents the best fit, which corresponds to a value of $H_K = 1.7$ kOe, that gives an effective in-plane anisotropy constant $K_1 \approx 52.9 \times 10^4$ erg/cm^3, together with $\alpha = 40^\circ$, consistent within the accuracy of sample alignment with the easy magnetization axis along [110].

The solid curve in Fig. 4(a) corresponds to the prediction of Eqs. (1) and (2), for the quoted value of the effective anisotropy field H_K with $\alpha = 40^\circ$, $\phi = 50^\circ$. The curve agrees well with the data for fields in excess of H_K, where a single domain structure is expected, and the maximum of $A(H)$ corresponds to the anisotropy field H_K. At $H < H_K$, the data deviate from the theoretical curve due to the dominant contribution of the domain-wall signal, which could not be unraveled from the signal of domains. Also the field dependence of the resonance frequency of Fig. 3(a) may be calculated without further adjustable parameters from the same minimization, by means of the projection of the magnetic field onto the local field, $\delta H = -H\cos(\theta_0 - \alpha)$ (dashed curve in the same figure).

We now turn to the field dependence of the resonance frequency in the $H_\perp$ geometry where we neglect the small in-plane magnetic anisotropy, so that the dc magnetic field $\mathbf{H}$, the magnetization $\mathbf{M}$, and the film normal $\mathbf{n}$ are coplanar. Thus the total energy is given by the expression

$$E = -HM_s \cos(\theta - \alpha) + K_u \sin^2\theta + 2\pi M_s^2 \cos^2\theta, \tag{3}$$

where α and θ are the angles of $\mathbf{H}$ and $\mathbf{M}_s$ from the film normal, respectively; K_u is an effective out-of-plane uniaxial anisotropy constant. The shift in the resonance field δH is given by projection of the magnetic and demagnetizing field onto the local field H_n at the Mn nuclei,

$$\delta H = 4\pi M_s \cos^2\theta_0 - H\cos(\theta_0 - \alpha). \tag{4}$$

The best fit of the reduced magnetization of Fig. 3(b) to the expression $M/M_s = \cos(\theta_0 - \alpha)$, where θ_0 is obtained minimizing Eq. (3), yields an effective anisotropy field value $H_A = 4\pi M_s + 2K_u/M_s = 7.86$ kOe. The term $2K_u/M_s$ represents a possible perpendicular uniaxial anisotropy, and, since we have measured the demagnetizing field $4\pi M_s = 7.79$ kOe by SQUID, the fit provides an estimated value $2K_u/M_s = 70$ Oe, corresponding to $K_u \leqslant 2.2 \times 10^4$ erg/cm^3, i.e., we may deduce the absence of a significant anisotropy with a symmetry axis normal to the plane of the film.

The shift of the resonance frequency was calculated from Eq. (4) using this H_A value. The solid curve in Fig. 3(a) represents this calculation where the only adjustable parameter is the estimated misorientation $\alpha = 5^\circ$. The agreement with the data is quite good. The same model predicts the field dependence of the FO NMR intensity displayed Fig. 4(b) (circles). Here too a good agreement is found for fields in excess of H_A.

This result confirms that our film behaves as a magnetically homogeneous sample also when selectively probing DE Mn. Furthermore, we have validated a method that could be applied to characterize magnetically thin films grown on magnetic substrates, such as $NdGaO_3$.

IV. CONCLUSION

^{55}Mn NMR detects two distinct signals from localized holes in the LSMO/STO interfaces and from the itinerant carriers of the upper layers of the films. The investigation of NMR spectra vs film thickness confirmed the presence of a dead layer (nonmetallic) at the interface with the substrate.

Although our main NMR result on LSMO/STO confirms qualitatively the findings of Bibes *et al.*[11] on LCMO/STO,

we notice two subtler differences. We do not detect evidence of an additional *nonmagnetic* insulating region at the interface, which was inferred from the thickness dependence of the f^{4+} intensity in LCMO/STO. Our LSMO/STO f^{4+} intensity is thickness independent. The Mn^{DE} frequency value shifts linearly[19] with charge carrier density and the variation with LCMO film thickness was attributed[11] to a corresponding dependence of the average density of carriers. We do not detect a similar change of the Mn^{DE} resonance frequency in LSMO/STO.

These differences may be related to specific properties of LCMO and LSMO, or else they may be related to sample preparation conditions. In both cases they indicate that NMR, in conjunction with magnetization measurements, is a very sensitive tool of the interface quality.

By examining the high field region of the field dependence of the NMR of LSMO/STO interfaces, the NMR response can be fitted to a simple model that allows independent determination of the anisotropy field in the films. Thus our results reveal agreement between the NMR and magnetization measurements. Specifically a comparison of the calculated and experimental field dependence of the ^{55}Mn NMR and SQUID results shows that magnetization rotation processes play a dominant role when the applied field exceeds the effective anisotropy field.

The marked difference in frequency shift between f^{4+} and f^{DE}, displayed in Fig. 3(a) indicates that the layers of the manganite films located close to the substrate are magnetically anisotropic, whereas the upper film layers are only slightly anisotropic. Does this indicate that the charge-separated dead layer is intrinsically more anisotropic than the DE manganite, or is the larger anisotropy simply an effect of the reduced thickness? We notice that for film thickness of few tens of nm or less the NMR enhancement factors of f^{4+} and f^{DE} coincide [Fig. 2(b)], suggesting that the anisotropy of the dead layer and of its overlayers becomes similar when their thickness is comparable. This is true also for the 8-nm film, which is almost exclusively composed of the dead layer.

This relatively small anisotropy of the charge-separated dead layer is somewhat surprising. However, it is well known that the similar insulating ferromagnetic state of manganites at slightly lower doping is composed of nanoscopic soft ferromagnetic clusters embedded in a canted antiferromagnetic background, which would have a much larger intrinsic magnetic anisotropy.[31] We take our observation as an indication of a strong coupling regime between the background and the nonpercolating ferromagnetic clusters, where the anisotropy of the latter must dominate. We remark that such a statement can only be made employing a selective probe such as NMR.

In conclusion we have demonstrated that ^{55}Mn NMR can be further exploited for probing the magnetic properties of films in an interface-selective way, which is a key issue of the design of spintronic junction devices.

ACKNOWLEDGMENTS

This work was supported by the PRIN project (Grant No. 2002023998), by the FIRB project (Grant No. RBNE017XSW) and by FISR project *Materiali e processi per sistemi nanostrutturati*. We acknowledge useful discussions with G. Asti, M. Solzi, M. Ghidini, and G. Guidi.

*Electronic address: sidorenko@fis.unipr.it

[1] S. Jin, T. H. Tiefel, M. McCormack, H. M. O'Bryan, L. H. Chen, R. Ramesh, and D. Schuring, Appl. Phys. Lett. **67**, 557 (1995).
[2] S. E. Lofland, S. M. Bhagat, H. L. Ju, G. C. Xiong, T. Venkatesan, R. L. Greene, and S. Tyagi, J. Appl. Phys. **79**, 5166 (1996).
[3] M. Ziese and S. P. Sena, J. Phys.: Condens. Matter **10**, 2727 (1998).
[4] M. Angeloni, G. Balestrino, N. Boggio, P. G. Medaglia, P. Orgiani, and A. Tebano, J. Appl. Phys. **96**, 6387 (2004).
[5] P. Lecoeur, P. L. Trouilloud, G. Xiao, A. Gupta, G. Q. Gong, and X. W. Li, J. Appl. Phys. **82**, 3934 (1997).
[6] J. Dho, Y. N. Kim, Y. S. Hwang, J. C. Kim, and N. H. Hur, Appl. Phys. Lett. **82**, 01434 (2003).
[7] K. Steenbeck, T. Habisreuther, C. Dubourdieu, and J. P. Senateur, Appl. Phys. Lett. **80**, 03361 (2002).
[8] Y. Suzuki, H. Y. Hwang, S.-W. Cheong, and R. B. van Dove, Appl. Phys. Lett. **71**, 140 (1997).
[9] L. M. Berndt, V. Balbarin, and Y. Suzuki, Appl. Phys. Lett. **77**, 02903 (2000).
[10] J. O'Donnell, M. S. Rzchowski, J. N. Eckstein, and I. Bozovic, Appl. Phys. Lett. **72**, 1775 (1998).
[11] M. Bibes, L. Balcells, S. Valencia, J. Fontcuberta, M. Wojcik, E. Jedryka, and S. Nadolski, Phys. Rev. Lett. **87**, 067210 (2001).
[12] J. Z. Sun, D. W. Abraham, R. A. Rao, and C. Eom, Appl. Phys. Lett. **74**, 3017 (1999).
[13] M. Bibes, S. Valencia, L. Balcells, B. Martínez, J. Fontcuberta, M. Wojcik, S. Nadolski, and E. Jedryka, Phys. Rev. B **66**, 134416 (2002).
[14] H. Yamada, Y. Ogawa, Y. Ishii, H. Sato, M. Kawasaki, H. Akoh, and Y. Tokura, Science **305**, 646 (2005).
[15] G. Allodi, A. Banderini, R. De Renzi, and C. Vignali, Rev. Sci. Instrum. **76**, 83911 (2005).
[16] E. A. Turov and M. P. Petrov, *Nuclear Magnetic Resonance in Ferro- and Antiferromagnets* (Halsted, New York, 1972).
[17] A. M. Portis and A. C. Gossard, J. Appl. Phys. **31**, S205 (1960).
[18] G. Matsumoto, J. Phys. Soc. Jpn. **29**, 606 (1970).
[19] G. Allodi, M. Cestelli Guidi, R. De Renzi, and M. W. Pieper, J. Magn. Magn. Mater. **242–245**, 639 (2002).
[20] P. A. Algarabel, J. M. De Teresa, J. Blasco, M. R. Ibarra, C. Kapusta, M. Sikora, D. Zajac, P. C. Riedi, and C. Ritter, Phys. Rev. B **67**, 134402 (2003).
[21] M. M. Savosta and P. Novák, Phys. Rev. Lett. **87**, 137204 (2001).
[22] T. Kubo, A. Hirai, and H. Abe, J. Phys. Soc. Jpn. **26**, 1094 (1969).
[23] M. M. Savosta, V. N. Krivoruchko, I. A. Danielenko, V. Y. Tarenkov, T. E. Konstantinova, A. V. Borodin, and V. N. Varyukhin, Phys. Rev. B **69**, 024413 (2004).
[24] A. J. Freeman, and R. E. Watson, in *Magnetism*, edited by G. T.

Rado and H. Suhl (Academic Press, New York, 1965), Vol. 2A, p. 168.

[25] L. B. Steren, M. Sirena, and J. Guimpel, Phys. Rev. B **65**, 094431 (2002).

[26] K. Postava, H. Jaffres, A. Schuhl, F. Nguyen Van Dau, M. Goiran, and A. R. Fert, J. Magn. Magn. Mater. **172**, 199 (1997).

[27] E. Gu, J. A. C. Bland, C. Daboo, M. Gester, L. M. Brown, R. Ploessl, and J. N. Chapman, Phys. Rev. B **51**, 3596 (1995).

[28] A. Berger, A. Inomata, J. S. Jiang, J. E. Pearson, S. D. Bader, and K. Dahmen, J. Appl. Phys. **89**, 7466 (2001).

[29] A. Berger, A. Inomata, J. S. Jiang, J. E. Pearson, and S. D. Bader, Phys. Rev. Lett. **85**, 4176 (2000).

[30] K. Le Dang, P. Veillet, C. Chappert, R. F. C. Farrow, R. F. Marks, and D. Weller, Phys. Rev. B **48**, R14023 (1993).

[31] M. Hennion, F. Moussa, G. Biotteau, J. Rodríguez-Carvajal, L. Pinsard, and A. Revcolevschi, Phys. Rev. Lett. **81**, 1957 (1998).